J Fluoresc (2010) 20:843–850
DOI 10.1007/s10895-010-0627-z

ORIGINAL PAPER

Fluorescence Enhancement of the Silver Nanoparticales – Curcumin - Cetyltrimethylammonium Bromide-nucleic Acids System and its Analytical Application

Haiping Zhou · Xia Wu · Wei Xu · Jinghe Yang · Qiuxia Yang

Received: 21 May 2009 / Accepted: 8 February 2010 / Published online: 4 March 2010

Abstract It is found that silver nanoparticles (AgNPs) can further enhance the fluorescence intensity of curcumin (CU) - cetyltrimethylammonium bromide (CTAB) – nucleic acids and improve its anti-photobleaching activity. Under optimum conditions, the enhanced fluorescence intensity is proportion to the concentration of nucleic acids in the range of 2.0×10^{-8}–1.0×10^{-6} g mL^{-1} for fish sperm DNA (fsDNA), 2.0×10^{-8}–1.0×10^{-6} g mL^{-1} for calf thymus DNA (ctDNA), 1.0×10^{-8}–1.0×10^{-6} g mL^{-1} for yeast RNA (yRNA), and their detection limits ($S/N=3$) are 8.0 ng mL^{-1}, 10.5 ng mL^{-1} and 5.8 ng mL^{-1}, respectively. This method is used for determining the concentration of DNA in actual sample with satisfactory results. The interaction mechanism is also studied.

Keywords Curcumin · Cetyltrimethylammonium bromide · Silver nanoparticales · Nucleic acids

Introduction

Recently, metal nanoparticles have aroused worldwide research interests due to their unique physical and chemical properties which lead to many potential applications. For example, they can be used in optoelectronics [1], biological labeling [2–4], biological and chemical sensing [5, 6]. Especially, AgNPs have shown excellent antimicrobial activity compared to other available silver antimicrobial agents such as silver nitrate or silver sulfadiazine [7]. They could protect cells against HIV-1 infection and promote wound healing [8]. And they also have important function in anti-inflammation, anti-virus and anticancer [9, 10]. As we know, DNA is an attractive template because of its large aspect ratio (length/diameter), well-defined sequences of DNA base, a variety of superhelix and a high affinity for metal cations. So with chemical reduction, silver cations could form metallic nanowires following the contour of the DNA template [11]. Recently, it has been demonstrated that silver nanocluster [12] and silver nanoring [13] can be formed through a DNA-templated process. In addition, the determination of nucleic acids using AgNPs has aroused abroad interest and attention [14–16].

Curcumin (CU), the major active component of turmeric, is widely used as food coloring additive and as coloring agent in yellow mustards, cosmetics, pharmaceuticals, and hair dyes. Traditionally it has been in the practice for the treatment of common cold, skin diseases, wound healing etc [17]. CU is attracting remarkable continuing interest because of its antioxidant, anti-inflammatory, antimicrobial, antiamyloid and antitumor properties [18, 19]. Recently, extensive research has revealed that CU can both prevent and treat cancer [20–22].

As we know, under the strong light irradiating, the fluorescence intensities of dyes continue to decrease. To resolve this problem, scientists have put forward an improved method. In this study, the fresh-prepared AgNPs was utilized to improve the anti-photobleaching activity of the CU-CTAB-nucleic acids system and

H. Zhou · X. Wu (✉) · W. Xu · J. Yang
Key Laboratory of Colloid and Interface Chemistry (Shandong University), Ministry of Education, School of Chemistry and Chemical Engineering, Shandong University, Jinan 250100, China
e-mail: wux@sdu.edu.cn

Q. Yang (✉)
School of Chemistry and Chemical Engineering, University of Jinan, Jinan 250022, China
e-mail: chm_yangqx@ujn.edu.cn

further enhanced its fluorescence intensity. In this paper, a new method for nucleic acids determination was developed. The experiments indicated that the enhanced fluorescence intensity was in proportion to the concentration of nucleic acids. The interaction mechanism of the system was also studied by the transmission electronic microscopy (TEM), resonance light scattering and circular dichroism spectra, fluorometric method, zeta potentials and UV spectrometry.

Experiment

Chemicals

Stock solutions of nucleic acids (1.0×10^{-4} g mL^{-1}) were prepared by dissolving commercial fsDNA (Sigma), ctDNA and yRNA (Beijing Baitai Co., China) in 0.05 mol L^{-1} sodium chloride solutions. Silver nanoparticles prepared: A stock solution of silver nanoparticles (2.0×10^{-4} g mL^{-1}) was prepared by dissolving 0.0158 g of $AgNO_3$ in 40 mL of 0.22 μm-filtered doubly distilled water, 2 mL sodium citrate (1%) was added slowly in above $AgNO_3$ solution by heating at 86°C with stirring for 30 min, the solution color changed gradually from colorless to olivine, diluting to 50 mL finally.Stock standard solution (1.0×10^{-3} mol l^{-1}) of CU was made by dissolving 0.0368 of CU in ethanol and diluting to 50 ml and then diluted to 1.0×10^{-4} mol L^{-1} with ethanol as the working solution. Above solutions were stored at 0–4°C. A stock solution of CTAB (1.0×10^{-2} mol L^{-1}) was prepared by dissolving 1.8222 g CTAB in 500 mL volumetric flask with water. Briton-Robinson (BR, 4.0×10^{-2} mol L^{-1}) buffer solutions were prepared in such a way that 0.575 mL glacial acetic acid, 0.685 mL phosphoric acid and 0.6183 g boric acid dissolved in water then by dilution with water to 500 mL, and adjusted between 2.2 and 5.0 with 2.0 mol/L NaOH solution. All the chemicals used were of analytical reagent grade and double-distilled water was used throughout.

Apparatus

The resonance light scattering spectra and fluorescence spectra were measured using a LS-55 spectrofluorimeter (PE, USA). All absorption spectra were measured on a U-4100 spectrophotometer (Hitachi, Japan). TEM images were measured on JEM-100 CXII Transmission Electron Microscope (JEOL, Japan). All CD spectra were collected on a J-810S Circular Dichroism Spectrometer (JASCO, Japan). Zeta potentials (ζ) were measured with a JS94H micro-television electrophoretic instrument (Powereach, Shanghai). All pH measurements were made with a Delta 320-S acidity meter (Mettler Toledo, Shanghai).

Procedure

To a 10 mL colorimetric tube, the solutions were added in the following order: BR, CTAB, CU, AgNPs and fsDNA. The mixture was diluted to 5 mL with water and allowed to stand for 5 min. The excitation and emission wavelengths were 396 and 518 nm, respectively. The excitation and emission slits were both 10 nm with a scan speed of 500 nm/min. The enhanced fluorescence intensity of the system is represented as $\Delta I = I_f - I_0$. Here I_f and I_0 are the fluorescence intensity of the system with and without nucleic acids.

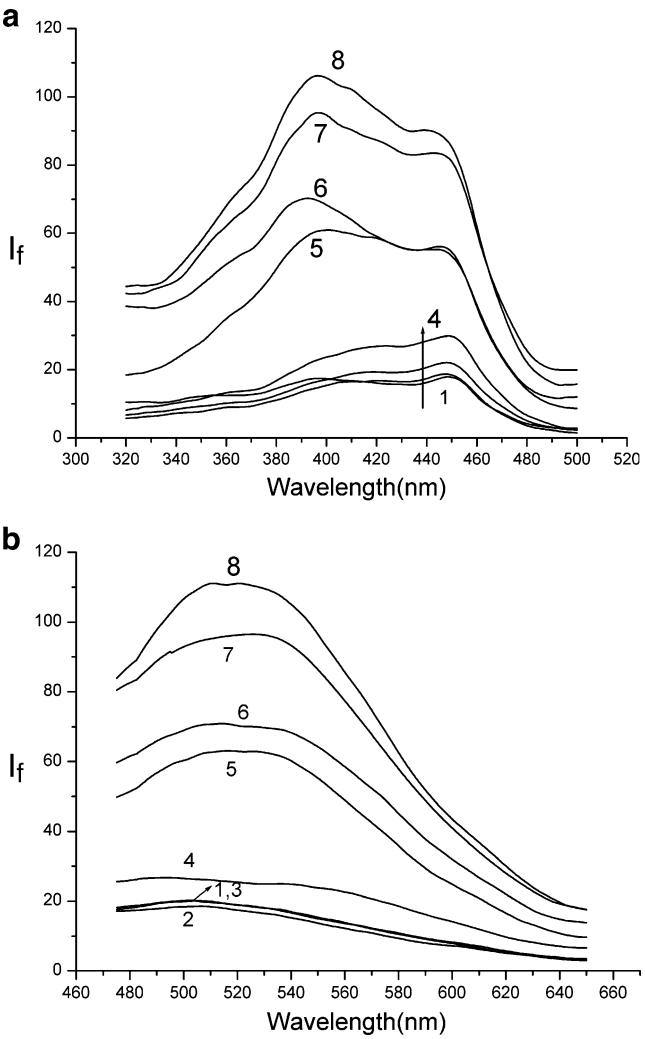

Fig. 1 **a** Excitation spectrum. **b** Emission spectrum. 1. CU; 2. CU - CTAB; 3. CU-CTAB-AgNPs; 4. CU-CTAB-fsDNA; 5. CU-CTAB-AgNPs-ctDNA; 6. CU-CTAB-AgNPs- fsDNA; 7. CU-CTAB-AgNPs- yRNA; Conditions: CTAB: 8.0×10^{-5} mol L^{-1}; AgNPs: 1.6×10^{-6} g mL^{-1}; CU: 1.0×10^{-6}molL^{-1}; fsDNA: 1.0×10^{-6} g mL^{-1}; ctDNA: 1.0×10^{-6} g mL^{-1}; yRNA: 1.0×10^{-6} g mL^{-1}; BR: 4.0×10^{-3} mol L^{-1}

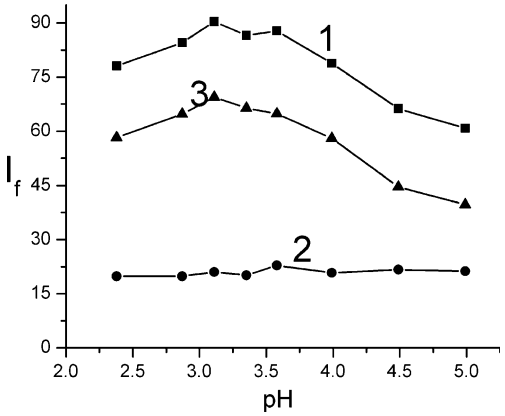

Fig. 2 Effect of pH. 1. I_f 2. I_0 3.ΔI. Conditions: CTAB: 8.0×10^{-5} mol L^{-1}; AgNPs: 1.6×10^{-6} g mL^{-1}; CU: 1.0×10^{-6}molL^{-1}; fsDNA: 1.0×10^{-6} g mL^{-1}; BR: 4.0×10^{-3}mol L^{-1}

Result and discussion

Fluorescence spectra

From Fig. 1, it could be seen that the fluorescence intensities of the CU, CU-CTAB, CU-CTAB-AgNPs systems are all weak. The emission peak of CU is at about 510 nm, and its two excitation peaks are at 396 nm and 440 nm, respectively. The fluorescence intensity of CU is enhanced by nucleic acids in the presence of CTAB, and further enhanced in the presence of AgNPs. Furthermore, it could also be seen that the maximum emission peak of CU shifts from 510 to 518 nm in the system of AgNPs-CU-CTAB- nucleic acids, which indicates that there exists the interaction among CU, nucleic acids, CTAB and AgNPs. It is apparent that the enhanced fluorescence intensity under the excitation of 396 nm is higher than that under the excitation of 440 nm. So we chose 396 nm as the excitation wavelength and 518 nm as the emission wavelength in our further studies.

Effect of pH and the choice of buffer solution

It could be seen from Fig. 2 that ΔI value reaches the maximum at the pH 3.1, so pH 3.1 is used for subsequent work. Experimental results indicated that different kinds of buffers have different effects on the ΔI (%) of the system. The ΔI (%) for BR, citric acid -K_2HPO_4, hexamethylenetetramine (HMTA) - HCl, citric acid- sodium citrate and NaAc–HAc are 100, 85.8, 11.93, 94.9 and 91.2, respectively. It could be seen that BR is the most suitable buffer. Further studies demonstrate that the optimum volume of 4.0×10^{-2} mol L^{-1} BR is 0.5 ml.

Effect of surfactants

The effects of different surfactants on the system are studied. The results show that anionic surfactants such as sodium dodecyl benzene sulfonate (SDBS) and sodium laurel sulfate (SLS) and nonionic surfactant Triton X-100 had little effect on the system. But cationic surfactants, such as cetyltrimethyl ammonium bromide (CTAB), cetylpyridine bromide (CPB), have obvious enhancement on the fluorescence. From above results, it could be seen that the biggest ΔI was obtained in AgNPs-CU-fsDNA-CTAB system. So CTAB was used in the system.

The effect of CTAB concentration is also tested and shown in Fig. 3a. It is found that the ΔI of this system reaches a maximum when the concentration of CTAB is 8.0×10^{-5} mol L^{-1}. So 8.0×10^{-5} mol L^{-1} is chosen for further research.

Figure 3b show that the variation of the electrical conductivity with CTAB concentration. The critical micelle concentration (CMC) is obtained from the interception of conductivity lines above and below the apparent CMC. The

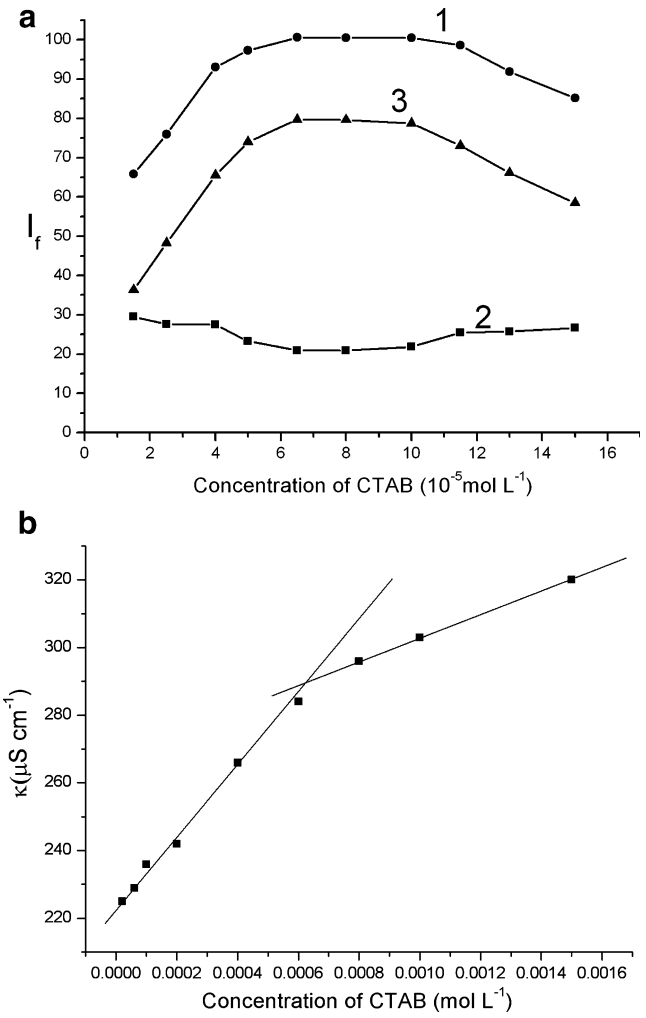

Fig. 3 **a** Effect of the concentration of CTAB. 1. I_f 2. I_0 3.ΔI. **b** The conductivity of the system. Conditions: AgNPs: 1.6×10^{-6} g mL^{-1}; CU: 1.0×10^{-6}mol L^{-1}; fsDNA: 1.0×10^{-6} g mL^{-1}; BR: 4.0×10^{-3} mol L^{-1}

concentration 6.2×10^{-4} mol L^{-1} may be regarded as the CMC of CTAB in this system. So it can be seen that the selected concentration of CTAB is below its CMC, which show that CTAB exists as the pre-micelle or monomer in the studied system.

Effect of AgNPs concentration

From Fig. 4, it could be seen that the value of ΔI of the system remains the maximum when the concentration of AgNPs is in range of 1.6×10^{-6}–4.0×10^{-6} g mL^{-1}. And when the concentration of AgNPs is 1.6×10^{-6} g mL^{-1}, I_f/I_0 (%) value of this system reaches a maximum and the value of I_0 is lower. Considering the effect of regent blank of the system, 1.6×10^{-6} g mL^{-1} AgNPs is chosen for further experiment.

Effect of CU concentration

The effect of the concentration of CU is tested and shown in Fig. 5. It could be seen that the ΔI of this system reached a maximum when the concentration of CU is 1.0×10^{-6} mol L^{-1}, So 1.0×10^{-6} mol L^{-1} is chosen for further experiment.

Adding sequence and signal stability

The effect of adding sequence and signal stability on the fluorescence intensity are also investigated. The experiments indicate that the addition sequence of reagents affects the ΔI of the system, and the order of BR, CTAB, CU, AgNPs and fsDNA is the best.

Under the optimum condition, the effect of time on the fluorescence intensity is studied. The results show that the ΔI reaches a maximum at 5 min after all the reagents added, and it remains stable for over 55 min.

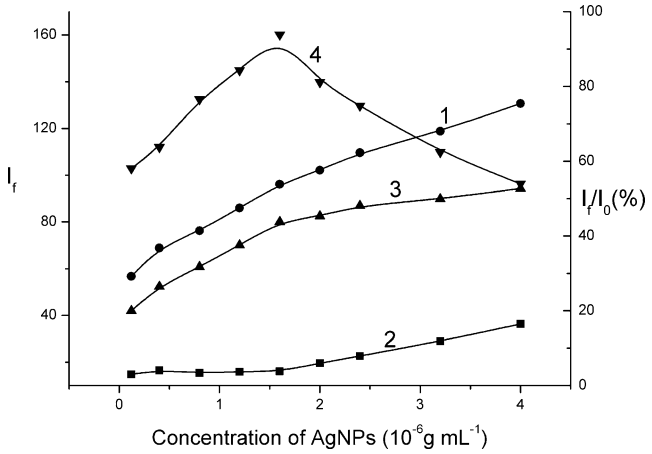

Fig. 4 Effect of AgNPs. 1. I_f 2. I_0 3.ΔI 4. I_f/I_0. Conditions: CTAB: 8.0×10^{-5} mol L^{-1}; CU: 1.0×10^{-6}molL^{-1}; fsDNA: 1.0×10^{-6} g mL^{-1}; BR: 4.0×10^{-3} mol L^{-1}

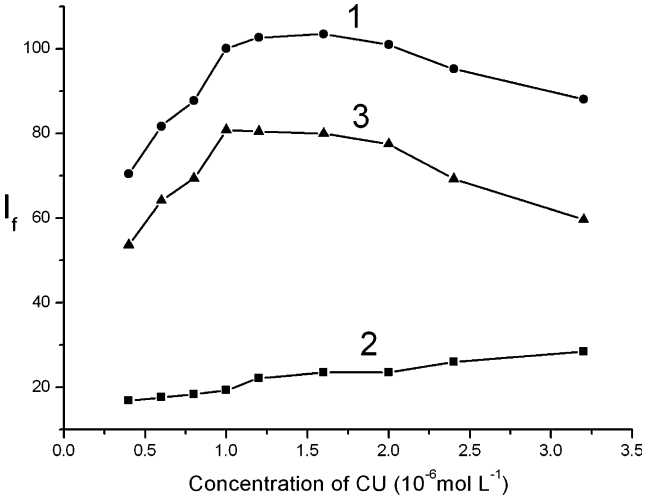

Fig. 5 Effect of CU. 1. I_f 2. I_0 3.ΔI. Conditions: CTAB: 8.0×10^{-5} mol L^{-1}; AgNPs: 1.6×10^{-6} g mL^{-1}; fsDNA: 1.0×10^{-6} g mL^{-1}; BR: 4.0×10^{-3} mol L^{-1}

The fluorescence photobleaching property of the system is monitored under continuous irradiation of the excitation light (λex=396 nm) with a pulsed-xenon flash lamp as the source lamp with 20 kW for 8 μs duration. The result indicated that after adding AgNPs to the CU-CTAB-fsDNA system, the time of the fluorescence intensity maintained with relative error less than ±5% is lengthened from 7 to 33 min. Therefore, the system of AgNPs-CU-CTAB-fsDNA appears highly stable against fluorescence photobleaching property.

Effect of foreign substances

The interference of foreign substances is shown in Table 1. It is found that most of the amino acids, metal ions and nucleotides have little effect on the determination of fsDNA within ±5% relative error.

Analytical applicayion

The calibration graph and detection limits

Under the optimum conditions defined, the calibration graphs for fsDNA , ctDNA and yRNA were obtained (Table 2) and showed that there was a linear relationship between the ΔI of the system and the concentration in the range of 2.0×10^{-8}–1.0×10^{-6} g mL^{-1} for fsDNA, 2.0×10^{-8}–1.0×10^{-6} g mL^{-1} for ctDNA, 1.0×10^{-8}–1.0×10^{-6} g mL^{-1} l for yRNA, their detection limits (S/*N*=3) are 8.0 ng mL^{-1}, 10.5 ng mL^{-1} and 5.8 ng mL^{-1} respectively.

Table 1 Interference from foreign substance

Foreign substance	Concentration coexisting $\times 10^{-6}$mol L^{-1}	Change of ΔI (%)
K^+	40	−5.9
Na^+	30	−5.0
Mg^{2+}	35	−6.7
NH_4^+	6.0	+3.7
Ca^{2+}	15	4.8
Fe^{3+}	2.0	−3.8
Cu^{2+}	1.5	−6.3
L-Cys	12	6.7
Pro	8.0	+3.6
L-His	40	−4.5
L-Asp	5.0	5.6
L-phe	8.0	5.7
GMP	4.0	5.7
AMP	4.0	5.5
CMP	3.0	5.3
UMP	2.0	5.3
TMP	1.0	5.4
BSA	3 μg mL^{-1}	−3.0
HSA	3 μg mL^{-1}	−4.8

Conditions: CTAB: 8.0×10^{-5} mol L^{-1}; AgNPs: 1.6×10^{-6} g mL^{-1}; CU: 1.0×10^{-6} mol L^{-1}; fsDNA: 4.0×10^{-7} g mL^{-1}; BR: 4.0×10^{-3} mol L^{-1}

Determination of actual sample

An actual sample of plasmid DNA (offered by School of Life Science, Shandong University) is tested by the standard addition method. The content of DNA in the sample is 7.0×10^{-4} g mL^{-1}, which is obtained by using a Biophotometer(Eppendorf Co.). The sample is diluted 7000 times and determined by this proposed method, the mean value of the three measurements was 6.8×10^{-4} g mL^{-1} and the relative standard deviation was 1.3% (n=3). Hence, the proposed method was suitable for the determination of trace amount of nucleic acids in this sample.

Interaction mechanism of the system

Assembly behavior of AgNPs

The resonance light scattering (RLS) technique is available to provide some insight into the process responsible for the formation of the complex. It can be seen form Fig. 6 that the RLS intensity of CU-CTAB is weak, but the RLS spectrum is obviously enhanced in the present of AgNPs, which indicates that the complex of AgNPs-CU-CTAB is formed. And when fsDNA is added to AgNPs-CU-CTAB complex, the RLS intensity is greatly enhanced. According to the RLS theory, it is concluded that the larger complex of AgNPs-CU-CTAB-fsDNA is formed and the size of nanoparticles are enlarged.

The TEM images of AgNPs(a), AgNPs -CTAB-CU(b) and AgNPs-CTAB -CU-fsDNA(c) show in Fig. 7. From

Table 2 Analytical parameters of this method

Nucleic acid	Linear range(g mL^{-1})	r[a]	LOD[b](ng mL^{-1})
fsDNA	2.0×10^{-8}–1.0×10^{-6}	0.997	8.0
ctDNA	2.0×10^{-8}–1.0×10^{-6}	0.995	10.5
yRNA	1.0×10^{-8}–1.0×10^{-6}	0.999	5.8

[a] Correlation coefficient [b] limit of detection

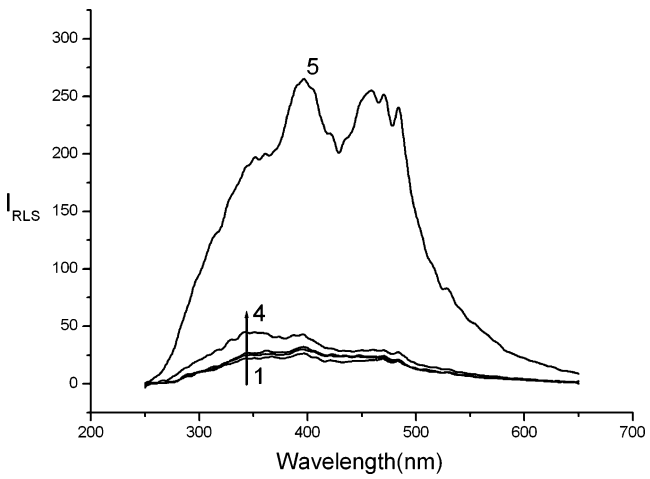

Fig. 6 Resonance light scattering spectra of the system. 1. CU 2. CU-AgNPs 3.CU-CTAB 4. CU-CTAB-AgNPs 5. CU-CTAB-fsDNA-AgNPs. Conditions: CTAB: 8.0×10^{-5} mol L^{-1}; AgNPs: 1.6×10^{-6} g mL^{-1}; CU: 1.0×10^{-6}mol L^{-1}; fsDNA: 1.0×10^{-6} g mL^{-1}; BR: 4.0×10^{-3} mol L^{-1}

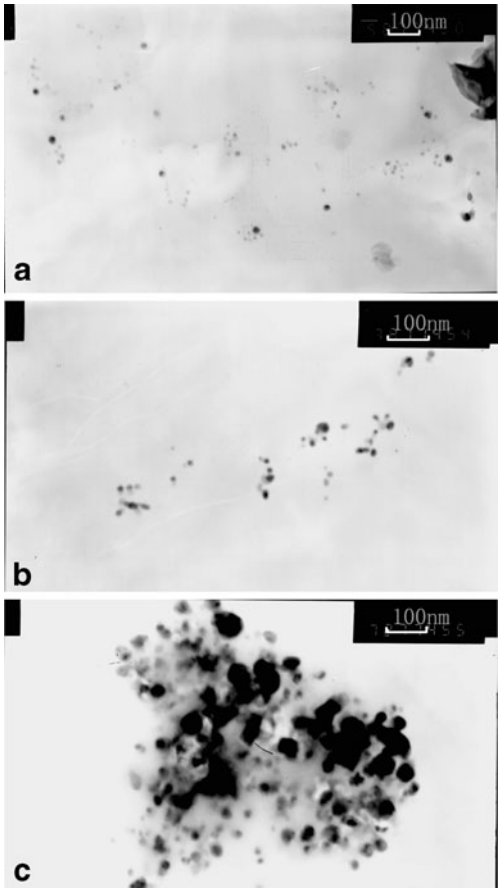

Fig. 7 a,b,c Transmission electronic microscopy. **a**. AgNPs **b**. CU-CTAB-AgNPs **c**. CU-CTAB-fsDNA-AgNPs. Conditions: CTAB: 1.0×10^{-4} mol L^{-1}; AgNPs: 1.6×10^{-5} g mL^{-1}; CU: 1.0×10^{-5}mol L^{-1}; fsDNA: 1.0×10^{-5} g mL^{-1}; BR: 4.0×10^{-3}mol L^{-1}

Fig. 7(a), it can be seen that AgNPs are spherical in shape and the size of the AgNPs is about 20 nm, and they are well dispersed. When CU and CTAB are added to AgNPs solution, nanoparticles congregate partly and their size are not obviously changed (Fig. 7b). However, after adding fsDNA to AgNPs-CU-CTAB system, it can be seen that nanoparticles congregate greatly and their size are about 40 nm (Fig. 7c).

Interaction between CU-CTAB-AgNPs and fsDNA

Curcumin is a diferuloyl mechane molecule containing two ferulic acid residues joined by a methylene bridge. Due to its β-diketone moiety, it undergoes keto-enol tautomerism. It is well known that in solution and solid phase, curcumin exists entirely as enol form CU [23, 24], which has a symmetrical conjugated π-bond system. Figure 8 exhibits that CU has a maximum absorption peak at about 425 nm and a shoulder peak at about 365 nm, this band corresponds to an electronic dipole allowed π-π*, and intramolecular charge-transfer transition. It can be seen that AgNPs have weak absorption peak at 423 nm corresponding to their plasmon resonance absorption, which reflects that the formation of AgNPs (inset Fig. 8). Under adding both CTAB and AgNPs into CU solution, this system appear the highly broadened and red-shifted band of CU, which is considered to be attributed to the exciton coupling between electronic dipole transition moments of the feruloyl parts rotated around the central methylene group [25, 26]. In other words, AgNPs-CTAB complex is combined on the centre of CU. Comparison of the absorption spectrum of AgNPs-CU-CTAB (vs. CU-CTAB) to that of AgNPs-CU-CTAB-fsDNA (vs. CU-CTAB-fsDNA) demonstrate that a red shift and broadening in absorption, the peak of the system shifts from 380 nm to 423 nm. This indicates the later formed larger aggregation [27]. That is in accordance with the result of TEM.

From Fig. 9, we can find that the ζ of CU-CTAB-AgNPs is about +133 mV in BR buffer. With the addition of fsDNA, ζ of the system decreased. We think that it is attributed to the binding of positive charged CU-CTAB-AgNPs with negatively charged fsDNA. These indicate that there exist electrostatic interactions among CU-CTAB-AgNPs and fsDNA.

The CD-spectra in the UV range can be used to monitor the conformational transition of DNA [28, 29]. In order to explain the interaction between fsDNA and AgNPs-CU-CTAB system, the CD spectra of the system are studied and shown in Fig. 10. It is known that a positive Cotton effect at 278 nm corresponding to base stacking, and a negative Cotton effect at 248 nm corresponding to helicity in the CD spectrum of fsDNA. Upon adding CTAB to fsDNA solution, the positive peak decreases obviously in height with a red shift of both the positive and the negative peaks. We think that CTAB could induce the structural change of base stacking and helicity of fsDNA. After adding AgNPs and CU to CTAB-fsDNA system, the positive peak shifts to shorter wavelength and increases a little and the negative peak shifts to longer wavelengths, which prove that the conformation of fsDNA is changed for the synergistic effect of CTAB, AgNPs and CU.

Fluorescence enhancement mechanism

The ratio of emission intensities for first and third vibronic bands of pyrene monomer (I_1/I_3) is a well established parameter, which reflects the polarity changes of a system experienced by the pyrene probe [30]. A low value reflects a lower polar environment than a high value. The experiments indicate that the I_1/I_3 values of the pyrene in the systems of fsDNA, CTAB-fsDNA and AgNPs-CTAB-fsDNA are 1.73, 1.50 and 1.42, respectively. This indicates that AgNPs-CTAB-fsDNA provide a microenvironment with low polarity for CU, resulting in the enhancement of the fluorescence intensity of CU in the AgNPs-CU-CTAB-

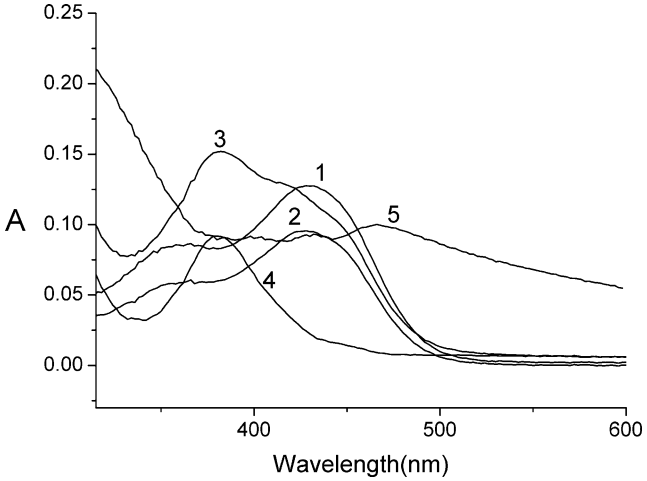

Fig. 8 Absorption spectra of the system. 1. CU 2. CU-CTAB 3. CU-CTAB-AgNPs 4. AgNPs-CU-CTAB (vs. CU-CTAB) 5. AgNPs-CU-CTAB-fsDNA (vs. CU-CTAB-fsDNA). Conditions: CTAB: 8.0×10^{-5} mol L^{-1}; AgNPs: 1.6×10^{-6} g mL^{-1}; CU: 1.0×10^{-6}mol L^{-1}; fsDNA: 1.0×10^{-6} g mL^{-1}; BR: 4.0×10^{-3} mol L^{-1}

fsDNA system. Moreover, the microviscosity of the microenvironment could be estimated using the fluorescence polarization of fluorescence probe, according to Perrin equation [31]. A large value reflects a larger microviscosity than a low value. The experimental results show that the fluorescence polarizations of the systems of CU-fsDNA, CU-fsDNA-CTAB and CU-fsDNA-CTAB-AgNPs are 0.379, 0384 and 0.456, respectively. This indicates that fsDNA-CTAB-AgNPs provide a hydrophobic environment with high microviscosity for CU. In addition, the hydrophobic environment of AgNPs-CTAB-fsDNA system could also prevent the collision between complex and water and decrease the energy loss of the CTAB-CU-AgNPs-fsDNA system. Thus, the fluorescence quantum yield is improved and the fluorescence intensity of CU system is significantly enhanced.

As discussed above, upon adding fsDNA to the AgNPs-CU-CTAB system, the fluorescence intensity is strongly enhanced and nanoparticles congregate greatly and their sizes are enlarged. According to the previously studies [27], we concluded that an optimum distance between CU and the surface of the AgNPs, resulting from the synergistic effect of CTAB and fsDNA, is another reason of the fluorescence enhancement and anti-photobleaching activity improvement. And more detail investigation on the fluorescence enhancement mechanism of the system is still in progress.

Conclusions

AgNPs can further enhance the fluorescence intensity of CU-CTAB-nucleic acids and improve its anti-photobleaching activity. Based on this, a simple and sensitive method for the determination of nucleic acid has been established. The detection limits is down to 10^{-9} g mL^{-1} level. The results for the determination of DNA in actual samples are satisfactory. The interaction mechanism investigation indicates the larger aggregation of CU-CTAB-AgNPs-fsDNA is formed through electrostatic interaction and hydrophobic interaction. In addition, the reasons for the fluorescence enhancement of the system of AgNPs-CU-CTAB-fsDNA may be that an optimum hydrophobic environment with low polarity and large microviscosity for CU is provided by AgNPs-CTAB-fsDNA system and an optimum distance between CU and the surface of the AgNPs, resulting from the synergistic effect of CTAB and fsDNA.

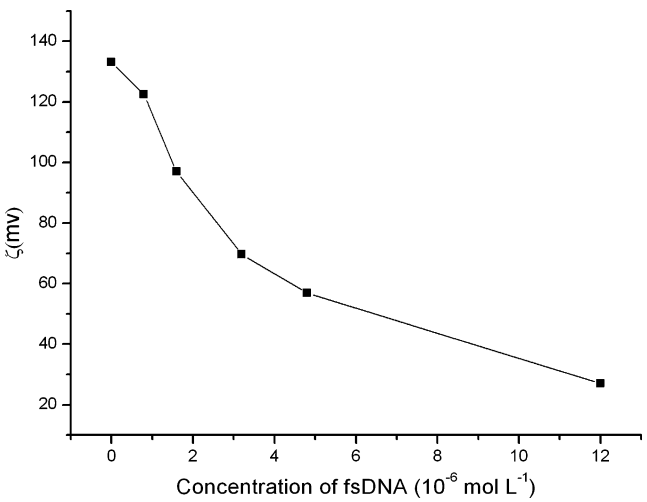

Fig. 9 The ζ of the system. Conditions: CTAB: 8.0×10^{-5} mol L^{-1}; AgNPs: 1.6×10^{-6} g mL^{-1}; CU: 1.0×10^{-6}mol L^{-1}; BR: 4.0×10^{-3} mol L^{-1}

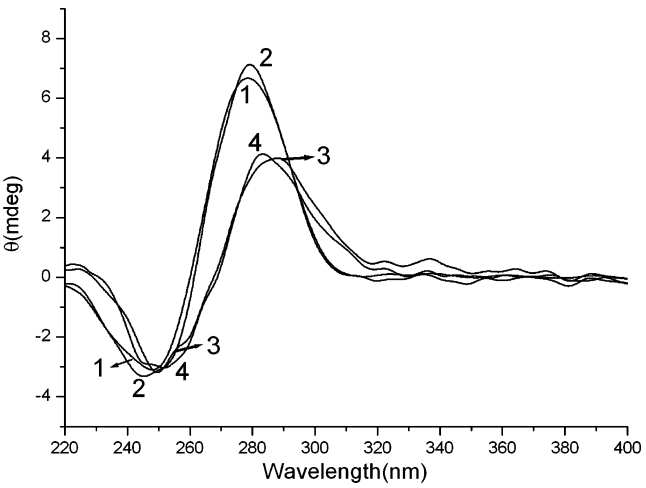

Fig. 10 The CD spectra of AgNPs-CU-CTAB and fsDNA system. 1. fsDNA; 2. AgNPs-CU-fsDNA; 3. CTAB-fsDNA; 4.AgNPs-CU-CTAB-fsDNA. Conditions: CTAB: 8.0×10^{-5} mol L^{-1}; AgNPs: 1.6×10^{-6} g mL^{-1}; CU: 1.0×10^{-6} mol L^{-1}; fsDNA: 5.0×10^{-5} g mL^{-1}; BR:4.0×10^{-3} mol L^{-1}

Acknowledgment This work is supported by Natural Science Foundations of China (20575035) and Shandong Province (Z2008B04).

References

1. Dick LA, McFarland AD, Haynes CL, Duyne RPV (2002) Metal Film over Nanosphere (MFON) Electrodes for Surface-Enhanced Raman Spectroscopy (SERS): improvements in Surface Nanostructure Stability and Suppression of Irreversible Loss. J Phys Chem B 106:853–860. doi:10.1021/jp013638l
2. Nicewarner-Pena SR, Freeman RG, Reiss BD, He L, Pena DJ, Walton ID, Cromer R, Keating CD, Natan MJ (2001) Submicrometer metallic barcodes. Science 294:137–141. doi:10.1126/science.294.5540.137
3. Geerts H, Brabander MD, Nuydens R (1991) Nanovid microscopy. Nature 351:765–766. doi:10.1038/351765a0
4. Hainfeld JF, Powell RD (2000) New frontiers in gold labeling. J Histochem Cytochem 48:471–480
5. Tian N, Zhou ZY, Sun SG, Ding Y, Wang ZL (2007) Synthesis of tetrahexahedral platinum nanocrystals with high-index facets and high electro-oxidation activity. Science 316:732–735. doi:10.1126/science.1140484
6. Zhang JG, Gao Y, Alvarez-Puebla RA, Buriak JM, Fenniri H, Buriak JM (2006) Synthesis and SERS properties of nanocrystalline gold octahedra generated from thermal decomposition of $HAuCl_4$ in block copolymers. Adv Mater 18:3233–3237. doi:10.1002/adma.200601368
7. Yin HQ, Langford R, Burrel RE (1999) Comparative evaluation of the antimicrobial activity of ACTICOAT antimicrobial barrier dressing. J Burn Care Rehabil 20:195–200. doi:10.1097/00004630-199905000-00006
8. Tian J, Wong KY, Ho CM, Lok CN, Yu WY, Che CM, Chiu JF, Tam PH (2007) Topical delivery of silver nanoparticles promotes wound healing. Chem Med Chem 2:129–136. doi:10.1002/cmdc.200600171
9. Elechiguerra JL, Burt JL, Morones JR, Camacho-Bragado A, Gao X, Lara HH, Yacaman MJ (2005) Interaction of silver nanoparticles with HIV-1. J Nanobiotechnol 3:6. doi:10.1186/1477-3155-3-6
10. Braun E, Eichen Y, Sivan U, Ben-Yoseph G (1998) DNA-templated assembly and electrode attachment of conducting silver wire. Nature 391:775–778. doi:10.1038/35826
11. Xiong YJ, Xie Y, Wu CZ, Yang J, Li ZQ, Xu F (2003) Formation of silver nanowires through a sandwiched reduction process. Adv Mater 15:405–408. doi:10.1002/adma.200390092
12. Petty JT, Zheng J, Hud NV, Dickson RM (2004) DNA-templated Ag nanocluster formation. J Am Chem Soc 126:5207–5212. doi:10.1021/ja031931o
13. Sun LL, Wei G, Song YH, Liu ZG, Wang L, Li Z (2006) Fabrication of silver nanoparticles ring templated by plasmid DNA. Appl Surf Sci 252:4969–4974. doi:10.1016/j.apsusc.2005.07.016
14. Pan Q, Zhang RY, Bai YF, He NY, Lu ZH (2008) An electrochemical approach for detection of specific DNA-binding protein by gold nanoparticle-catalyzed silver enhancement. Anal Biochem 375:179–186. doi:10.1016/j.ab.2007.12.006
15. Zheng JH, Wu X, Wang MQ, Ran DH, Xu W, Yang JH (2008) Study on the interaction between silver nanoparticles and nucleic acids in the presence of cetyltrimethylammonium bromide and its analytical application. Talanta 74:526–532. doi:10.1016/j.talanta.2007.06.014
16. Bao P, Frutos AG, Greef C, Lahiri J, Muller U, Peterson TC, Warden L, Xie XY (2002) High-sensitivity detection of DNA hybridization on microarrays using resonance light scattering. Anal Chem 74:1792–1797. doi:10.1021/ac0111964
17. Chattopadhyay I, Biswas K, Bandyopadhyay U, Banerjee RK (2004) Banerjee turmeric and curcumin: biological actions and medicinal applications. Curr Sci 87:44–53
18. Maheshwari RK, Singh AK, Gaddipati J, Srimal RC (2006) Multiple biological activities of curcumin: a short review. Life Sci 78:2081–2087. doi:10.1016/j.lfs.2005.12.007
19. Ono K, Hasegawa K, Naike H, Yamada MJ (2004) Curcumin has potent anti-amyloidogenic effects for Alzheimer's beta-amyloid fibrils in vitro. J Neurosci Res 75:742–750. doi:10.1002/jnr.20025
20. Balasubramanian KJ (2006) Molecular orbital basis for yellow curry spice curcumin's prevention of Alzheimer's disease. Agric Food Chem 54(10):3512–3520. doi:10.1021/jf0603533
21. Park SY, Kim DS (2002) Discovery of natural products from Curcuma longa that protect cells from beta-amyloid insult: a drug discovery effort against Alzheimer's disease. J Nat Prod 56:1227–1231. doi:10.1021/np010039x
22. Shishodia S, Potdar P, Gairola CG, Aggarwal BB (2003) Curcumin (diferuloylmethane) down- regulates cigarette smoke-induced NF- kappaB activation through inhibition of IkappaBalpha kinase in human lung epithelial cells: correlation with suppression of COX-2, MMP-9 and cyclin D1. Carcinogenesis 24:1269–1279. doi:10.1093/carcin/bgg078
23. Khopde SM, Priyadarsini KI, Palit DK, Mukherjee T (2000) Effect of solvent on the excited state photophysical properties of curcumin. Photochem Photobiol 72:625–631. doi:10.1562/0031-8655(2000)072<0625:EOSOTE>2.0.CO;2
24. Tonnesen HH, Karlsen J, Mostad A (1982) Structural studies of curcuminoids. 1. The crystal structure of curcumin. Acta Chem Scand B 36:475–479. doi:10.3891/acta.chem.scand.36b-0475
25. Zsila F, Bikadi Z, Simonyi M (2003) Molecular basis of the Cotton effects induced by the binding of curcumin to human serum albumin. Tetrahedron Asymmetry 14:2433–2444. doi:10.1016/S0957-4166(03)00486-5
26. Pedersen U, Rasmussen PB, Lawesson SO (1985) Synthesis of naturally occurring curcuminoids and related-compounds. Liebigs Ann Chem 8:1557–1569. doi:10.1002/jlac.198519850805
27. Sokolov K, Chumanov G, Cotton TM (1998) Enhancement of molecular fluorescence near the surface of colloidal metal films. Anal Chem 70:3898–3905. doi:10.1021/ac9712310
28. Zhang ZL, Huang WM, Tang JL, Wang EK, Dong SJ (2002) Conformational transition of DNA induced by cationic lipid vesicle in acidic solution: spectroscopy investigation. Biophys Chem 97:7–16. doi:10.1016/S0301-4622(02)00006-6
29. Zhou YL, Li YZ (2004) Studies of interaction between poly (allylamine hydrochloride) and double helix DNA by spectral methods. Biophys Chem 107:273–281
30. Nakajima A (1983) A study on the system of pyrene and β-cyclodextrin in aqueous solution utilizing the intensity enhancement phenomenon. Spectrochim Acta A 39(10):913–915
31. Shinitzky M, Barenholz Y (1978) Fluidity parameters of lipid regions determined by fluorescence polarization. Biochem Biophys Acta 515(4):367–394